DOI 10.5012/bkcs.2010.31.8.2151

Photophysical Properties of Chlorotriethylphosphinegold(I)

Jun-Gill Kang,* Yong-Kwang Jeong, Sung-Il Oh, Hyun-Jun Kim, Changmoon Park, and Edward R. R. Tiekink†

*Department of Chemistry, Chungnam National University, Daejon 305-764, Korea. *E-mail: jgkang@cnu.ac.kr*
†Department of Chemistry, University of Malaya, 50603 Kuala Lumpur, Malaysia
Received March 8, 2010, Accepted June 4, 2010

Spectroscopic and quantum mechanical studies of the Et_3PAuCl complex were performed to characterize the effect of aurophilicity on the optical properties. When excited with UV light at low temperature, the crystalline complex produced a deep luminescence in both the blue (high-energy) and red (low-energy) regions of the spectrum. The intensity of the low-energy luminescence was markedly reduced in the powdered state and quenched in the solution state. Time-dependent density functional theory (TD-DFT) calculations on electronic structures of both the ground and excited states of aggregates $[Et_3PAuCl]_n$ (n = 1 - 3) indicated that the low-energy luminescence was attributable to Au-centered transitions, which are significantly affected by aurophilic interactions. By contrast, the high-energy luminescence appeared to be independent of the state of the complex and was strongly associated with the charge transfer from Cl to Au.

Key Words: Chlorotriethylphosphinegold(I), Optical properties, Aurophilic interactions, Au-centered transitions, Charge transfer

Introduction

The luminescence properties of organophosphinegold(I) complexes have been extensively investigated and have become an important sub-discipline in the study of gold chemistry.[1-3] For organophosphinegold(I) halides containing bulky organophosphine ligands, such as R_3PAuX (R = phenyl and *o*-tolyl), there is significant variety in their luminescence properties. When excited with UV light, these complexes produce emission bands in the 350 - 500 nm region with a low-energy shoulder. The observed luminescence has been attributed to intra-ligand transitions,[4] metal-centered transitions,[5] or ligand-to-metal charge transfer transitions.[6] For complexes containing small organophosphine ligands, such as $[(Me_2Ph)PAuX]_n$ and (TPA)AuX (TPA = 1,3,5-triaza-7-phosphaadamantabe, X = Cl, Br and I), whereby supramolecular association occurs *via* aurophilic (Au···Au) interactions to form dimeric (in the case of bromide and iodide) or trimeric (in the case of chloride) complexes, an additional low-energy emission band is observed in the region 550 - 700 nm. The low-energy band is due to phosphorescence from the gold-based $\sigma(p) \rightarrow \sigma^*$ (s,d) excitation,[7] and its appearance was strongly associated with Au···Au aurophilicity. The energies of Au···Au bonds, measured in the range of 29 - 46 kJ mol^{-1}, are comparable with strong hydrogen bonds.[8] Accordingly, aurophilic interactions are very important in determining the molecular and crystal structure of compound and have clear implications for the optical properties in phosphinegold halides, the theme of the present report.

Notwithstanding the foregoing, a large variety of gold complexes in addition to phosphinegold halides have been investigated for correlations between the molecular and supramolecular structure and the observed photophysical properties. Species receiving recent attention include metal-organic complexes of varying coordination number, having different counterions, featuring aurophilic interactions, being subject to mechanochemical stress (piezochromic luminescent materials), or bearing ligands having their own fluorescent activity.[1,9] Increasingly important in this context are organogold species, with gold in both the +I and +III oxidation states.[10] An important motivation for on-going studies of this sort is their application in biochemistry, where the luminescence of gold compounds with aurophilic forming capacity has been exploited to develop sensors of alkali and alkaline earth ions, as well as of transition metals.[11]

The present study was undertaken to investigate the optical properties of a prototype complex, specially Et_3PAuCl, in which Au···Au interactions have been observed in the crystal structure, as indicated by the Au···Au bond distance of 3.568(2) and 3.615(2) Å.[12] These distances are at the upper end of the generally accepted range of intermolecular Au···Au interactions (see Figure 3 in ref. 8), but as shown in this study, are important in influencing the photophysical properties. Complementing the experimental procedures, TD-DFT calculations[13] of the molecular orbitals and excited states of $[Et_3PAuCl]_n$ (n = 1 - 3) were performed to characterize the absorbing and emitting states. TD-DFT has been proven to be a practical and useful method in estimating the binding energy[14] of the gold atom and the potential-energy surface of gold clusters.[15] The electronic structures of $[Et_3PAuCl]_n$ are proposed and demonstrate the influence of aurophilic interactions. This work has relevance in delineating the luminescence properties of related mononuclear organophosphinegold(I) halides.

Experimental

Crystalline Et_3PAuCl and the Et_3P ligand, dissolved in THF, were purchased from Aldrich. The samples were used without further purification. Absorption spectra of solution samples were recorded on a Hitach U-4100 UV-vis spectrophotometer. For measurements of diffuse reflectance spectra, the samples were prepared by pulverizing a small amount (5 - 10 wt %) with $BaSO_4$. The diffuse reflectance spectra were recorded on

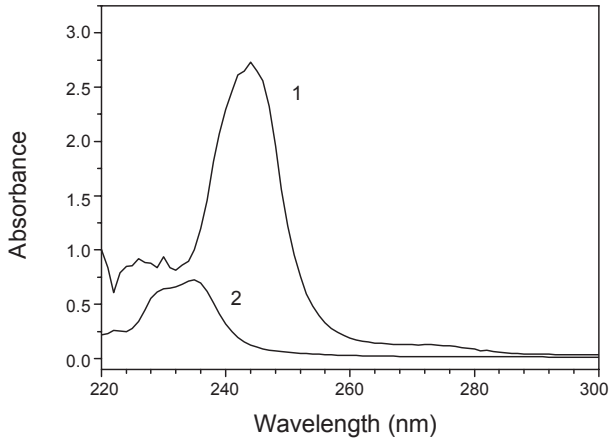

Figure 1. Absorption spectra of Et_3P (1, 0.10 M) and Et_3PAuCl (2, 3.0×10^{-4} M) in THF.

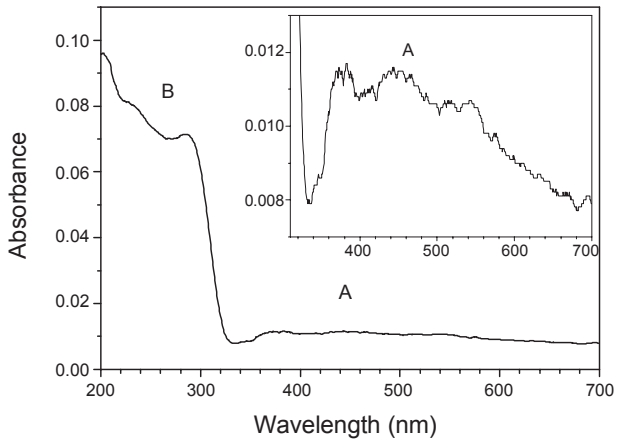

Figure 2. Diffuse reflectance spectrum of Et_3PAuCl at rt.

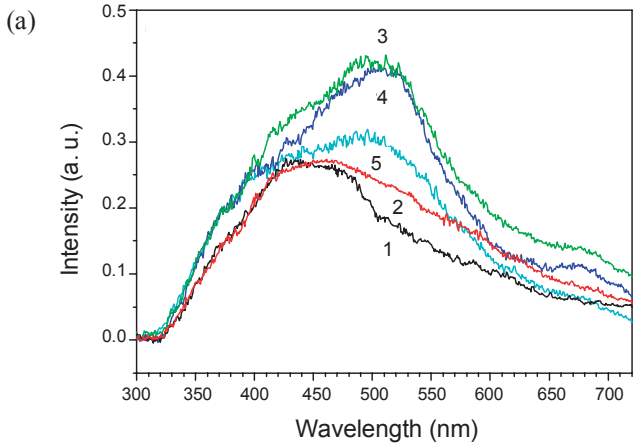

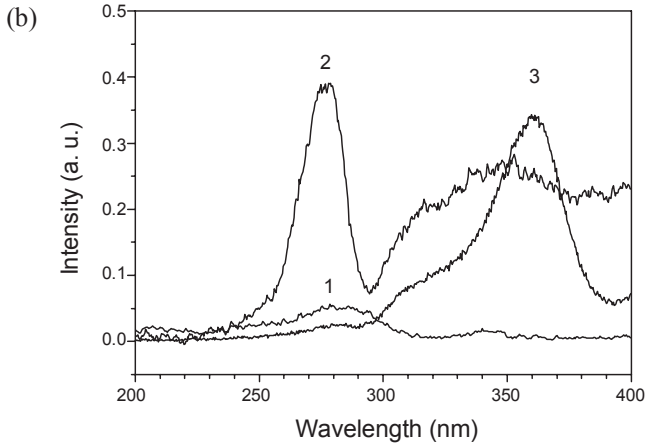

Figure 3. (a) Luminescence (λ_{exn} = 280 nm, 1: rt, 2: 150 K, 3: 90 K, 4: 70 K, 5: 10 K) and (b) excitation (λ_{ems} = 1: 680 nm, 2: 500 nm, 3: 450 nm at 70 K) spectra of Et_3PAuCl.

a Shimadzu UV-3101PC spectrophotometer equipped with an integrating sphere attachment.

For measurements of luminescence and excitation spectra, microcrystalline samples were either placed on the cold finger of an Oxford CF-1104 cryostat using silicon grease (crystalline spectra), or were dissolved in THF in a quartz ampoule, degassed three times, then sealed (solution spectra). Excited light from either a He-Cd laser or an Oriel 1000-W Xe arc lamp, passed through an Oriel MS257 monochromator, was focused on the sample. The luminescence spectra were measured at a 90° angle with an ARC 0.5m Czerny-Turner monochromator equipped with a cooled Hamamatsu R-933-14 photomultiplier tube.

Results and Discussion

Optical properties.

Absorption and diffuse reflectance: The absorption spectra of the free ligand, Et_3P and the Et_3PAuCl complex, dissolved in THF, were measured in the 220 - 800 nm region. As shown in Figure 1, the absorption spectrum of the complex, with a band appearing at 235 nm (ε = 2400 M^{-1} cm^{-1}), was quite different from that of the free ligand. For the free ligand, two weak bands appeared at 244 nm (ε = 5.5 M^{-1} cm^{-1}) and 273 nm (ε = 0.26 M^{-1} cm^{-1}). These results suggested that the 235-nm band of the complex was associated with the Au(I) center.

The solid-state diffuse reflectance spectrum of Et_3PAuCl, measured at room temperature, was reproduced in the form of absorbance, *via* the Kubelka-Munk function.[16] As shown in Figure 2, a strong absorption band appeared below 300 nm, accompanied by a broad and weak band in the visible region. Hereafter, these are referred to as A- and B-absorption bands in the order of increasing energy. The A-absorption band appeared from 320 nm to 700 nm. Assuming that the main absorption peak was blue-shifted by ~ 50 nm when in solution, the strong B-absorption band in the solid-state would correspond to the 235-nm absorption band in the solution state.

Luminescence and excitation: The emission and excitation spectra of the complex in the crystalline state were measured at various temperatures (Figure 3(a)). At room temperature, the 280-nm excitation produced a weak and broad spectrum, with a complex spectral shape, spanning from 320 nm to 700 nm. With decreasing temperature, the intensity of the low-energy emission increased and became the maximum peak. At T = 70 K,

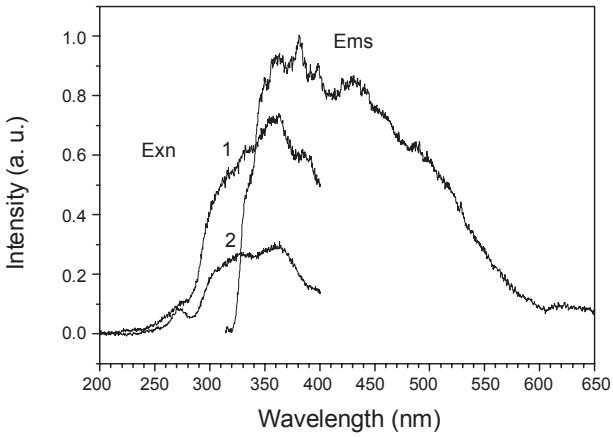

Figure 4. Luminescence (λ_{exn} = 280 nm) and excitation (λ_{ems} = 1 : 450 nm, 2 : 500 nm) spectra of powdered Et_3PAuCl at 70 K.

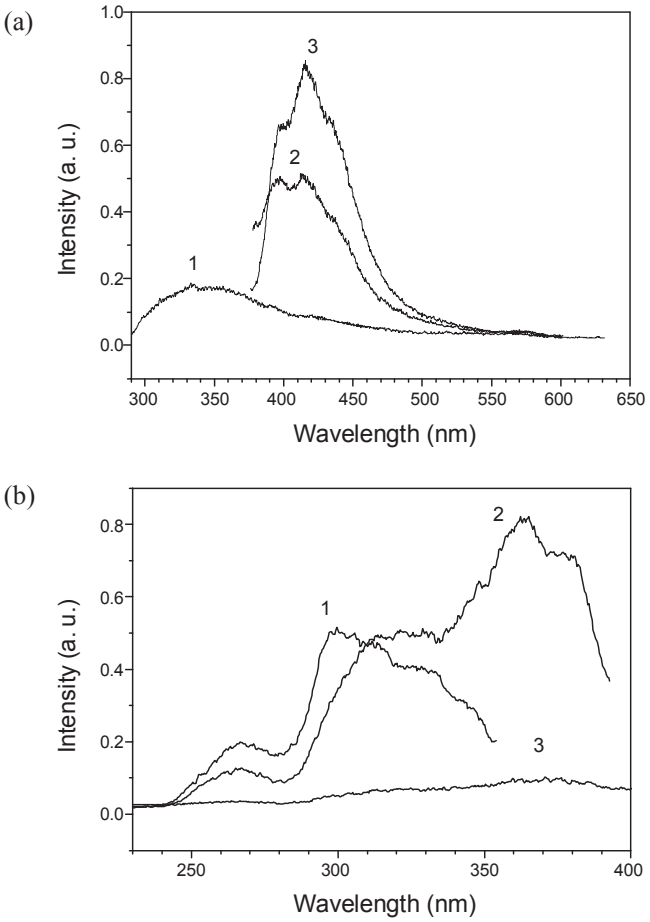

Figure 5. (a) Luminescence (λ_{exn} = 1 : 280 nm, 2 : 330 nm, 3 : 360 nm) and (b) excitation (λ_{ems} = 1 : 370 nm, 2 : 410 nm, 3 : 550 nm) spectra of Et_3PAuCl dissolved in THF (degassed).

the spectrum was resolved to four Gaussian components, peaking at 673 nm (w), 520 nm (p), 437 nm (s), and 375 nm (w): hereafter, these emission components were referred to as the E1, E2, E3, and E4 in the order of increasing the energy. The excitation spectra of the E1, E2 and E3 bands were also measured. As shown in Figure 3(b), the excitation spectrum showed

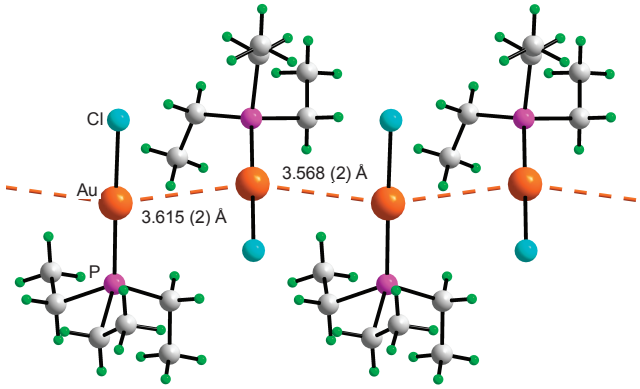

Figure 6. Supramolecular aggregation leading to a zigzag chain mediated by aurophilic (Au···Au) interactions in the crystal structure of Et_3PAuCl, after ref. 12.

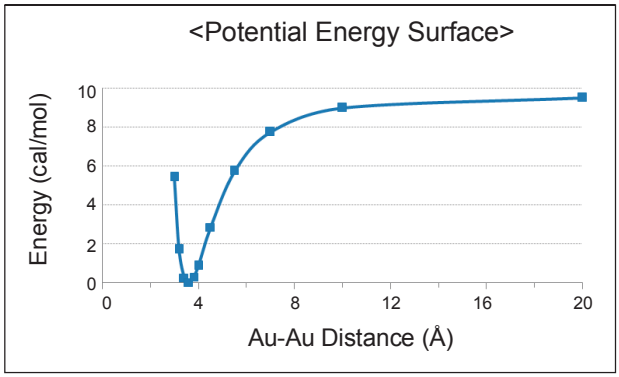

Figure 7. Potential energy surface of dimeric $[Et_3PAuCl]_2$, using the DFT/B3LYP level of theory with the LanL2DZ basis set.

two characteristic bands: low-energy and high-energy bands. The high-energy excitation band, peaking at 280, was well separated from the low-energy band appearing at ≥ 300 nm. Comparing the excitation spectra with the diffuse reflection spectrum, it is evident that the low-energy excitation band corresponds to the A-absorption band and the high-energy, 280-nm excitation band corresponds to the B-absorption band. It should be noted that the E1 emission was mainly produced *via* the B-band excitation at low temperature.

The effect of the states of the complex on the luminescence properties was also investigated by changing from a crystalline state to a powdered state and to a solution state. Figure 4 shows the luminescence spectrum measured for the complex after grinding into a powder. Compared with the crystalline state, the intensities of the E1 and E2 emission components were markedly reduced in the powder, suggesting that these low-energy (LE) emission components might be associated with the aurophilic interactions that are disrupted on grinding. To confirm whether the LE emissions were indeed associated with the aurophilic interaction, the luminescence properties of the complex were also investigated in degassed THF. As shown in Figure 5(a), the 280-nm excitation produced only weak high-

Table 1. Some calculated molecular orbitals of $[Et_3PAuCl]_n$ (n = 1, 2 and 3)

MO	n = 1					n = 2					n = 3				
	hartree	Au	Cl	P	C	hartree	Au	Cl	P	C	hartree	Au	Cl	P	C
*l*7	0.079	14	1	38	40	0.045	29		17	46	0.020	42	8	26	22
*l*6	0.063	17		10	54	0.029	54	2	10	29	0.016	39	7	28	24
*l*5	0.054	20		19	53	0.016	59	8	29	3	0.013	40	1	22	32
*l*4	0.042	20		13	52	0.008	27	1	19	49	−0.002	37	2	17	42
*l*3	0.017	54	7	34	4	0.002	24	1	19	53	−0.006	33	3	19	43
*l*2	−0.009	22	2	9	60	−0.003	34	4	20	40	−0.012	26	1	19	52
*l*1	−0.012	15	2	24	58	−0.017	20	2	20	57	−0.014	43		11	44
*h*1	−0.238	16	79		5	−0.238	32	68			−0.234	50	50		
*h*2	−0.238	15	77	3	4	−0.245	20	75		5	−0.239	21	79		
*h*3	−0.271	72	28			−0.246	22	73		5	−0.242	20	76		3
*h*4						−0.247	19	75	2	4	−0.243	20	77		3
*h*5						−0.260	83	18			−0.247	28	65		6
*h*6						−0.281	81	19			−0.248	29	63		8
*h*7											−0.252	72	29		
*h*8											−0.272	83	15		2

energy (HE) emissions (E3 and E4), with band shapes similar to those of the powder. The LE emissions were completely quenched in solution. These results indicated that the LE emissions are associated with the aurophilic interaction, which is absent in solution. The excitation spectra of the HE emissions, on the other hand, exhibited bands similar to those of the crystalline state, corresponding to the A- and B-absorption bands. The O_2-purged solution of the complex also produced emission spectra similar to the degassed solution, indicating that the HE emissions were due to fluorescence. Finally, it is noted that Et_3P dissolved in THF produced a very weak emission, peaking at 355 nm. Accordingly, the LE bands of the complex, observed strongly in the crystalline state, are associated with the aurophilic interaction.

Ab initio calculations. To model the electronic structures and to understand the observed optical properties of Et_3PAuCl, quantum mechanical calculations were performed using DFT/B3LYP/LanL2DZ basis functions to determine the influence of the aurophilic interactions on the molecular orbitals of the complex. The starting model was based on the previously published X-ray data[12] which showed two crystallographically distinct, but chemically similar molecules, in the asymmetric unit. In the crystal structure, these are associated into a supramolecular zigzag chain mediated by aurophilic, Au···Au, interactions (Figure 6). For the quantum mechanical calculations, three model systems (monomer, dimer, trimer) were investigated. Only the hydrogen atoms were optimized using DFT/B3LYP/LanL2DZ, and these optimized structures were then used for further calculations.

Aurophilic interaction: The potential energy surface between the two monomers was calculated using the optimized dimer. Single-point energies were calculated by varying the Au···Au distance with no further optimization of the geometry. As shown in Figure 7, the minimum energy of the aurophilic interaction was −9.49 kcal/mole corresponding to a Au···Au distance of 3.6 Å. This distance agrees well with the observed distances (Figure 6). Pyykkö derived a simple expression for the aurophilic attraction energy D_e (J) as a function of the equilibrium distance, R_e (pm):[8]

$$D_e = -\frac{(R_e b)}{n}(6.022 \times 10^{-2})$$

In this equation, n is a free parameter, and a and b are the so-called Herschbach-Laurie parameters. Taking a = 268 pm and b = −29 pm given for the $[(Ph_3AuX)_2]$ (X = F - I) model,[17] for $[Et_3PAuCl]_2$, n was calculated as 0.35.

MOs and electronic transitions: The results of the molecular orbital (MO) calculations using TD-DFT/B3LYP/LanL2DZ are listed in Table 1. For the monomer, the combinations of the $d_{x^2-y^2,xy}$ and $d_{yz,xz}$ orbitals of Au and the p_y and p_z orbitals of Cl resulted in the two-fold highest occupied orbitals (HOMOs), *h*1 and *h*2, respectively. The p orbitals of Cl contributed nearly 80%, indicating that these two HOMOs are mainly occupied by the lone-pair elections of Cl. The next HOMO, *h*3, is composed of another combination of the s and $d_{x^2-y^2,xy}$ orbitals of Au and the p_x orbital of Cl, with a very significant contribution from Au (as much as 72%) and a smaller contribution from Cl (p_x). The first two lowest unoccupied molecular orbitals (LUMOs), *l*1 and *l*2, consist of a linear combination of the s, p_y and p_z orbitals of carbon atoms as the main component, and the s and p_y orbitals of Au and the p_y orbital of P as minor components. The contributions of Au to the *l*1 and *l*2 LUMOs were only 15 and 22%, respectively. In contrast, the *l*3 LUMO consists of the s orbital of Au, with a contribution of 54%, and the s and p_x orbitals of P, with a contribution of 34%. The *l*3 LUMO corresponds to the σ*-antibonding between Au and P. The contributions of carbons, Au and P to the next four LUMOs are similar to those of the *l*1 and *l*2 LUMOs.

For the dimeric structure, each of the molecular orbitals of the monomeric structure is numerically doubled. As listed in Table 1, the first four *h*1 - *h*4 HOMOs are formed by a linear combination of the p_x, p_y, and/or p_z orbitals of two Cl atoms as the main contributors, with a minor contribution from the d orbitals of Au, mimicking the situation for the *h*1 and *h*2 HOMOs in the monomer. The *h*5 and *h*6 HOMOs are mainly composed of the s, $d_{yz,zx}$ and $d_{x^2-y^2,xy}$ orbitals of Au. As for the *l*1 and *l*2 LUMOs of the monomer, the first four *l*1 - *l*4 LUMOs of the dimer correspond to the σ*-bonding orbitals of two Et_3P ligands

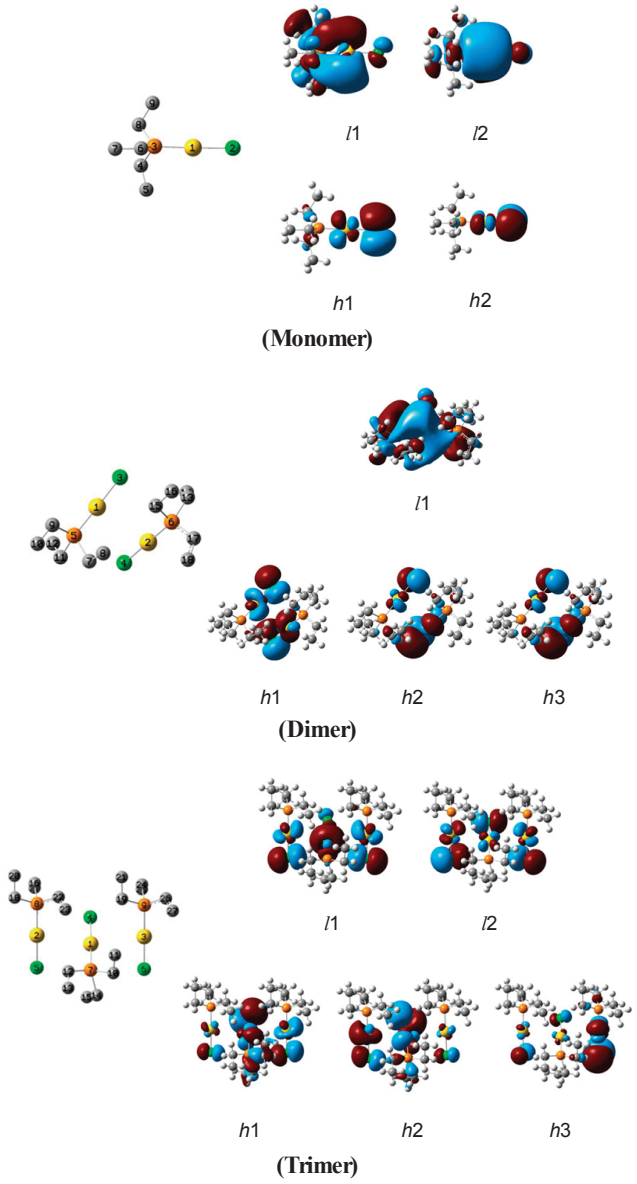

Figure 8. Contour plots of the molecular orbitals for $[Et_3PAuCl]_n$ (n = 1 - 3) involved in the A-band excitation and emission.

as the main contribution (over 40%), and the p orbitals of two Au atoms as the minor component with the contributions, with the contributions in the 20 - 34% range. The next two *l*5 and *l*6 LUMOs correspond to the *l*3 LUMO of the monomer. The s orbitals of the Au atoms are the major components of *l*5, and the s and p_x orbitals of Au are the main components for *l*6.

For the trimeric structure, the contribution of the s and d orbitals of Au atoms to the *h*1 HOMO increased, to as much as 50%, compared to the monomeric and dimeric species. Except for the *h*1 HOMO, similar trends in the nature of the MOs are evident as the number of units in the aggregates was systematically increased. The *h*2 - *h*6 HOMOs correspond to the lone-pair electrons of Cl atoms as main contributors, and the next four HOMOs, *h*7 - *h*10, consist largely of the s, $d_{yz,zx}$ and $d_{x^2-y^2,xy}$ orbitals of Au. The first six LUMOs, *l*1 - *l*6, are filled by the σ*-bonding orbitals of three Et_3P ligands and the p orbitals of Au

Table 2. Calculated excited states and predominant transitions for $[Et_3PAuCl]$

Excited states	eV	f	Predominant transition	Comment
(A-band)				
1A	5.18	0.001	*h*2 → *l*1	Cl(p)→Au(p)
2A	5.27	0.011	*h*1 → *l*1; *h*2 → *l*2	Cl(p)→Au(p)
3A	5.37	0.001	*h*1 → *l*2	Cl(p)→Au(p)
(B-band)				
4A	5.64	0.029	*h*2 → *l*2; *h*1 → *l*3	Cl(p)→Au(p, s)
5A	5.76	0.007	*h*2, *h*1→*l*3	Cl(p)→Au(s)
6A	5.83	0.034	*h*2, *h*1 → *l*3	Cl(p)→Au(s)
7A	6.17	0.065	*h*3 → *l*1	Au(s,d)→Au(p)
8A	6.39	0.062	*h*3 → *l*2	Au(s,d)→Au(p)

Table 3. Calculated excited states and predominant transitions for $[Et_3PAuCl]_2$

Excited states	eV	f	Predominant transition	Comment
(A-band)				
1A	5.21	0.020	*h*1 → *l*1	Cl(p)→Au(p)
2A	5.40	0.001	*h*4 → *l*1; *h*2 → *l*1	Cl(p)→Au(p)
3A	5.44	0.011	*h*2, *h*3 → *l*1	Cl(p)→Au(p)
4A	5.47	0.005	*h*3, *h*4 → *l*1	Cl(p)→Au(p)
(B-band)				
5A	5.62	0.002	*h*1 → *l*2	Cl(p)→Au(p)
6A	5.70	0.006	*h*3 → *l*2	Cl(p)→Au(p)
7A	5.76	0.005	*h*4 → *l*2; *h*1 → *l*3	Cl(p)→Au(p)
8A	5.78	0.019	*h*5 → *l*1	Au(s,d)→Au(p)
9A	5.82	0.029	*h*2 → *l*2; *h*5 → *l*1	Cl(p)→Au(p) Au(s,d)→Au(p)
10A	5.91	0.010	*h*2 → *l*3	Cl(p)→Au(p)
11A	5.94	0.018	*h*1 → *l*4	Cl(p)→Au(p)
12A	5.97	0.175	*h*1 → *l*5; *h*1 → *l*3; *h*5 → *l*1	Cl(p)→Au(s) Au(s,d)→Au(p)
13A	5.99	0.017	*h*3 → *l*3	Cl(p)→Au(p)

atoms as a main contribution, with the p orbitals of the P atoms as a minor component. The electron-density isocontours of the HOMOs and LUMOs calculated for $[Et_3PAuCl]_n$ (n = 1 - 3) are shown in Figure 8.

The calculated low-lying excited states and oscillator strengths of $[Et_3PAu]_n$ (n = 1 - 3) are listed in Tables 2 - 4. According to the energy gaps and the oscillator strengths, the excited states can be classified into two groups. As indicated in Table 2, for the monomer the first three excited states, 1A - 3A, are classified into group A and arise predominantly from transitions from the degenerate *h*1 and *h*2 HOMOs to the *l*1 and *l*2 LUMOs. The transitions from the X ground state to these excited states are responsible for the A-absorption band. However, the calculated oscillator strengths of these transitions are very low. Taking into account the partial MO components, the X → 1A - 3A transitions are associated with charge transfer from p(Cl) to p(Au). Although the σ*-antibonding orbitals of the Et_3P ligand are the main components in the *l*1 and *l*2 LUMOs, the

Table 4. Calculated excited states and predominant transitions for $[Et_3PAuCl]_3$

Excited states	eV	f	Predominant transition	Comment
(A-band)				
1A	5.27	0.039	$h1 \rightarrow l1$	Cl(p)→Au(p) Au(s,d)→Au(p)
2A	5.31	0.042	$h1 \rightarrow l2$; $h2 \rightarrow l2$	Cl(p)→Au(p) Au(s,d)→Au(p)
3A	5.42	0.015	$h3 \rightarrow l1$; $h2 \rightarrow l1$	Cl(p)→Au(p)
4A	5.46	0.001	$h4 \rightarrow l2$, $h3 \rightarrow l1$	Cl(p)→Au(p)
5A	5.47	0.005	$h2 \rightarrow l3$,	Cl(p)→Au(p)
6A	5.51	0.029	$h1 \rightarrow l2$; $h2 \rightarrow l2$; $h1 \rightarrow l3$	Cl(p)→Au(p) Au(s,d)→Au(p)
7A	5.55	0.019	$h4 \rightarrow l3$; $h4 \rightarrow l1$; $h4 \rightarrow l1$	Cl(p)→Au(p)
8A	5.57	0.019	$h1 \rightarrow l4$	Cl(p)→Au(p) Au(s,d)→Au(p)
(B-band)				
9A	5.62	0.005	$h6 \rightarrow l1$	Cl(p)→Au(p)
10A	5.63	0.015	$h5 \rightarrow l1$	Cl(p)→Au(p)
11A	5.67	0.115	$h7 \rightarrow l1$; $h4 \rightarrow l2$, $l3$; $h6 \rightarrow l1$	Au(s,d)→Au(p); Cl(p)→Au(p)
12A	5.69	0.025	$h5 \rightarrow l2$	Cl(p)→Au(p)
19A	5.88	0.106	$h2 \rightarrow l4$; $h7 \rightarrow l1$; $h6 \rightarrow l3$	Cl(p)→Au(p); Au(s,d)→Au(p)

p(Cl) → σ*(C) transitions are forbidden. The next five A states, 4A - 8A, can be included in group B. Among the calculated transitions, the oscillator strengths of the X → 7A and 8A transitions are the largest, with f = 0.065 and 0.062, respectively, and arise from the $h3 \rightarrow l1$ and $h3 \rightarrow l2$ transitions, respectively. Thus, these transitions correspond to Au-centered transitions are the main components of the B-absorption band, with the p(Cl) → s(Au) transitions also contributing. When the molecular aggregate is expanded from a monomer to a dimer and then to a trimer, the contributions of the Au orbitals to the $h1$ and $l1$ increase and the oscillator strengths of the transitions to some low-lying excited states increase (Tables 3 and 4). As indicated in Table 4, the 1A - 8A excited states can be classified into group A. For the A-band transitions, the summed oscillator strength was 0.013 for the monomer, 0.037 for the dimer, and 0.163 for the trimer. It should be noted that for the trimer, the first two excited states, 1A and 2A, arise from the combination of the p(Cl) → p(Au) and s,d(Au) → p(Au) transitions. It is suggested that low-lying excited states are associated with both the charge transfer transition from Cl to Au, and the Au-centered transitions, which are significantly affected by the oligomeric configuration mediated by aurophilic interactions. As the supramolecular association between the molecules increases *via* the aurophilic interaction, the oscillations of the Au-centered transitions increase and result in the low-energy luminescence.

Assignment of luminescence. For the monomeric structure of Et_3PAuCl, the A-band excited states are associated with the charge transfers from Cl to Au as a main component, and the direct transitions of Au as a minor component; the reverse is true for the B-band excited states. The aurophilic interaction significantly alters the nature of the A-band excited states. As the supramolecular association between the molecules increases, the contributions of the Au-centered transitions to the low-lying A-band excited states increase. The emitting centers responsible for the observed E1 (655 nm) and E2 (510 nm) emission components are strongly associated with the ^{1}[s,d(Au)] → ^{1}[p(Au)] transitions. By contrast, the high-lying A-band excited states, arising from charge transfer from Cl to Au, were not altered by the aurophilic interaction. The emitting centers for the observed 378 and 438 nm HE components arose from the [p(Cl)p(Au)]* electronic configurations.

Conclusions

The photophysical and conformational properties of the Et_3PAuCl complex were studied both experimentally and computationally. The crystalline complex excited with UV produced a broad luminescence from deep blue to deep red. The orange-red luminescence disappeared at high temperature, and in the powdered and solution states. This indicates that the low-energy luminescence is strongly associated with Au···Au interactions. The calculated aurophilic interaction of -9.49 kcal/mole (at an Au···Au distance of 3.6 Å) is sufficient to affect the photophysical properties. The results of TD-DFT and ZINDO calculations for $[Et_3PAu]_n$ (n = 1 - 3) suggested that the low-energy luminescence is attributed to the ^{1}[p*(Au)] → ^{1}[s,d(Au)] transition, whereas the high-energy luminescence is strongly associated with the ^{1}[p*(Cl)p*(Au)] excited states.

Acknowledgments. This research was supported by National Research Foundation (2009-0073199). J-GK, Y-KJ, S-IO and H-JK acknowledge the fellowships of the BK 21 program.

References

1. Forward, J. M.; Fackler, J. P., Jr.; Assefa, Z. *Optoelectronic Properties of Inorganic Compounds*; Roundhill, D. M., Fackler, J. P., Jr., Eds.; Plenum Press; New York, 1999; Ch. 6.
2. Tiekink, E. R. T.; Kang, J.-G. *Coord. Chem. Rev.* **2009**, *253*, 1627.
3. (a) Yam, V. W.-W.; Cheng, E. C.-C. *Top. Curr. Chem.* **2007**, *281*, 269. (b) Yam, V. W.-W.; Cheng, E. C.-C. *Chem. Soc. Rev.* **2008**, *37*, 1806.
4. (a) Larsen, L. J.; McCauley, E. M.; Weissbart, B.; Tinti, D. S. *J. Phys. Chem.* **1995**, *99*, 7218. (b) Bardaji, M.; Laguna, A.; Vicente, J.; Jones, P. G. *Inorg. Chem.* **2001**, *40*, 2675. (c) Osawa, M.; Hoshino, M.; Akita, M.; Wada, T. *Inorg. Chem.* **2005**, *44*, 1157.
5. (a) King, C.; Wang, J.-C.; Khan, M. N. I.; Fackler, J. P., Jr. *Inorg. Chem.* **1989**, *28*, 2145. (b) King, K.; Khan, M. N. I.; Staples, R. J.; Fackler, J. P., Jr. *Inorg. Chem.* **1992**, *31*, 3236. (c) Pawlowski, V.; Kunkely, H.; Vogler, A. *Inorg. Chim. Acta* **2004**, *357*, 1309.
6. (a) Kang, J.-G.; Park, C.; Tiekink, E. R. T. *Bull. Korean Chem. Soc.* **2006**, *27*, 299. (b) Hanna, S. D.; Khan, S. I.; Zink, J. I. *Inorg. Chem.* **1996**, *35*, 5813. (c) Bardaji, M.; Laguna, A.; Vicente, J. *Inorg. Chem.* **2001**, *40*, 2675.
7. Weissbart, B.; Toronto, D. V.; Balch, A. L.; Tinti, D. S. *Inorg. Chem.* **1996**, *35*, 2490.
8. Pyykkö, P. *Angew. Chem. Int. Ed.* **2004**, *43*, 4412.
9. (a) Osawa, M.; Kawata, I.; Igawa, S.; Tsuboyama, A.; Hashizume, D.; Hoshino, M. *Eur. J. Inorg. Chem.* **2009**, 3708. (b) Crespo, O.; Concepción Gimeno, M.; Laguna, A.; Kulcsar, M.; Silvestru, C. *Inorg. Chem.* **2009**, *48*, 4134. (c) Mullice, L. A.; Thorp-Greenwood, F. L.; Laye, R. H.; Coogan, M. P.; Kariuki, B. M.; Pope, S.

J. A. *Dalton Trans*. **2009**, 6836. (d) Balch, A. L. *Angew. Chem. Int. Ed*. **2009**, *48*, 2641. (e) Takemura, Y.; Takenaka, H.; Nakajima, T.; Tanase, T. *Angew. Chem. Int. Ed*. **2009**, *47*, 2157. (f) Elbjeirami, O.; Gonser, M. W. A.; Stewart, B. N.; Bruce, A. E.; Bruce, M. R. M.; Cundari, T. R.; Omary, M. A. *Dalton Trans.* **2009**, 1522.

10. (a) Gao, L.; Peay, M. A.; Partyka, D. V.; Updegraff, J. B.; Teets, T. S.; Esswein, A. J.; Zeller, M.; Hunter, A. D.; Gray, T. G. *Organometallics* **2009**, 28, 5669. (b) Au, V. K.-M.; Wong, K. M.-C.; Zhu, N.; Yam, V. W.-W. *J. Am. Chem. Soc*. **2009**, *131*, 9076. (c) Crespo, O.; Concepcóon Gimeno, M.; Laguna, A.; Ospino, I.; Aullon, G.; Oliva, J. M. *Dalton Trans*. **2009**, 3807.
11. (a) Abdou, H. E.; Mohamed, A. A.; Fackler, J. P.; Burini, A.; Galassi, R.; Lopez-de-Luzuriaga, J. M.; Olmos, M. E. *Coord. Chem. Rev*. **2009**, *253*, 1661. (b) Li, C.-K.; Lu, X.-X.; Wong, K. M.-C.; Chan, C.-L.; Zhu, N.; Yam, V. W.-W. *Inorg. Chem*. **2004**, *43*, 7421. (c) He, X.; Lam, W. H.; Zhu, N.; Yam, V. W.-W. *Chem. - Eur. J*. **2009**, *15*, 8842. (d) He, X.; Cheng, E. C.-C.; Zhu, N.; Yam, V. W.-W. *Chem. Commun.* **2009**, 4016.
12. Tiekink, E. R. T. *Acta Cryst*. **1989**, *C45*, 1233.
13. Gaussian 03, Revision C.02, Frisch, M. J.; Trucks, G. W.; Schlegel, H. B.; Scuseria, G. E.; Robb, M. A.; Cheeseman, J. R.; Montgomery, J. A., Jr.; Vreven, T.; Kudin, K. N.; Burant, J. C.; Millam, J. M.; Iyengar, S. S.; Tomasi, J.; Barone, V.; Mennucci, B.; Cossi, M.; Scalmani, G.; Rega, N.; Petersson, G. A.; Nakatsuji, H.; Hada, M.; Ehara, M.; Toyota, K.; Fukuda, R.; Hasegawa, J.; Ishida, M.; Nakajima, T.; Honda, Y.; Kitao, O.; Nakai, H.; Klene, M.; Li, X.; Knox, J. E.; Hratchian, H. P.; Cross, J. B.; Bakken, V.; Adamo, C.; Jaramillo, J.; Gomperts, R.; Stratmann, R. E.; Yazyev, O.; Austin, A. J.; Cammi, R.; Pomelli, C.; Ochterski, J. W.; Ayala, P. Y.; Morokuma, K.; Voth, G. A.; Salvador, P.; Dannenberg, J. J.; Zakrzewski, V. G.; Dapprich, S.; Daniels, A. D.; Strain, M. C.; Farkas, O.; Malick, D. K.; Rabuck, A. D.; Raghavachari, K.; Foresman, J. B.; Ortiz, J. V.; Cui, Q.; Baboul, A. G.; Clifford, S.; Cioslowski, J.; Stefanov, B. B.; Liu, G.; Liashenko, A.; Piskorz, P.; Komaromi, I.; Martin, R. L.; Fox, D. J.; Keith, T.; Al-Laham, M. A.; Peng, C. Y.; Nanayakkara, A.; Challacombe, M.; Gill, P. M. W.; Johnson, B.; Chen, W.; Wong, M. W.; Gonzalez, C.; Pople, J. A. Gaussian, Inc., Wallingford CT, 2004.
14. Cho, K.-H.; Joo, S.-W. *Bull. Korean Chem. Soc*. **2008**, *29*, 69.
15. Kim, K. H.; Kim, J. C.; Han, Y.-K *Bull. Korean Chem. Soc*. **2009**, *30*, 794.
16. Kortüm, G. *Reflectance Spectroscopy*; Springer-Verlag; New York, 1969.
17. Pyykkö, P.; Li, J.; Runeberg, N. *Chem. Phys. Lett*. **1994**, *218*, 133.